Luminescent Mononuclear and Binuclear Cyclometalated Palladium(II) Complexes of 6-Phenyl-2,2′-bipyridines: Spectroscopic and Structural Comparisons with Platinum(II) Analogues[1,2]

Siu-Wai Lai, Tsz-Chun Cheung, Michael C. W. Chan, Kung-Kai Cheung, Shie-Ming Peng,† and Chi-Ming Che*

Department of Chemistry, The University of Hong Kong, Pokfulam Road, Hong Kong

Received September 13, 1999

The mononuclear cyclometalated Pd(II) complexes [Pd(L^1)X] (HL^1 = 6-phenyl-2,2′-bipyridine; X = Cl, **1a**; Br, **1b**; I, **1c**), [Pd(L^1)PPh_3]$^+$ (**1d**), [Pd(L^{2-5})Cl] [**2a**−**5a**, HL^{2-5} = 4-(aryl)-6-phenyl-2,2′-bipyridine; aryl = phenyl (**2**), 4-chlorophenyl (**3**), 4-tolyl (**4**), 4-methoxyphenyl (**5**)] and the binuclear derivatives [$Pd_2(L^{1-5})_2(\mu$-dppm)]$^{2+}$ (**1e**−**5e**, dppm = bis(diphenylphosphino)methane) and [$Pd_2(L^1)_2(\mu$-dppC$_5$)]$^{2+}$, (**1f**, dppC$_5$ = 1,5-bis(diphenylphosphino)pentane) were prepared. The crystal structures of **1d**(ClO_4), **1e**(ClO_4)$_2$·DMF, and **2e**(ClO_4)$_2$ have been determined by X-ray crystallography. The magnitude of the Pd−Pd distances in **1e** and **2e** (3.230(1) and 3.320(2) Å, respectively) suggest minimal metal−metal interaction, although π-stacking of the aromatic ligands (interplanar separations 3.34 and 3.35 Å, respectively) is evident. All complexes display low-energy UV absorptions at $\lambda \sim$ 390 nm, which are tentatively assigned to ^{1}MLCT transitions; red shifts resulting from Pd−Pd interactions in the binuclear species are not apparent. The complexes in this work are non-emissive at 298 K, but the cationic derivatives exhibit intense luminescence at 77 K. The structured emissions of **1d** and **1f** in MeOH/EtOH glass (λ_{max} 467−586 nm) and all cationic species in the solid state (λ_{max} 493−578 nm) are assigned to intraligand excited states. Complexes **1e**−**5e** display dual emissions in MeOH/EtOH glass at 77 K, and the broad structureless bands at λ_{max} 626−658 nm are attributed to $\pi-\pi$ excimeric IL transitions. A comparison between the photophysical properties of Pd(II) and Pt(II) congeners is presented.

Introduction

The photophysics and photoreactivity of coordinatively unsaturated platinum(II) complexes[3] and their applications as luminescent sensors[4] are areas of considerable interest in inorganic photochemistry. Rich and diverse low-energy excited states, including IL (intraligand: $\pi \rightarrow \pi^*$), MLCT (metal-to-ligand charge transfer), [d$\sigma^* \rightarrow$ pσ], and [d$\sigma^* \rightarrow \pi^*$] (or MMLCT, metal−metal-to-ligand charge transfer), have been observed. Relatively scant attention has been focused upon the luminescent characteristics of palladium(II) complexes. Nevertheless, such investigations have been dominated by cyclometalated derivatives,[5−7] and reports comparing Pd(II) and Pt(II) analogues can yield information on electronic structures and excited states.[8,9] The ability of cyclometalated Pd(II) complexes to undergo DNA cleavage has been described.[10,11]

We have previously studied various aspects of luminescent cyclometalated Pt(II) complexes bearing substituted 6-phenyl-2,2′-bipyridine ligands.[1,2,4c,12] As part of a continuing program dedicated to luminescent d^8 systems, the preparation, crystal structures, and spectroscopic behavior of mono- and binuclear cyclometalated Pd(II) derivatives are presented. The correlation between Pd(II) and Pt(II) congeners has enabled evaluation of

* Corresponding author. Fax: +852 2857 1586. Email: cmche@hku.hk.

† Department of Chemistry, National Taiwan University, Taipei, Taiwan.

(1) Lai, S. W.; Chan, M. C. W.; Cheung, T. C.; Peng, S. M.; Che, C. M. *Inorg. Chem.* **1999**, *38*, 4046.
(2) Cheung, T. C.; Cheung, K. K.; Peng, S. M.; Che, C. M. *J. Chem. Soc., Dalton Trans.* **1996**, 1645.
(3) For example, see: (a) Roundhill, D. M.; Gray H. B.; Che, C. M. *Acc. Chem. Res.* **1989**, *22*, 55. (b) Houlding, V. H.; Miskowski, V. M. *Coord. Chem. Rev.* **1991**, *111*, 145. (c) Kunkely, H.; Vogler, A. *J. Am. Chem. Soc.* **1990**, *112*, 5625. (d) Cummings, S. D.; Eisenberg, R. *J. Am. Chem. Soc.* **1996**, *118*, 1949. (e) Sandrini, D.; Maestri, M.; Balzani, V.; Chassot, L.; von Zelewsky, A. *J. Am. Chem. Soc.* **1987**, *109*, 7720.
(4) For example, see: (a) Peyratout, C. S.; Aldridge, T. K.; Crites, D. K.; McMillin, D. R. *Inorg. Chem.* **1995**, *34*, 4484. (b) Kunugi, Y.; Mann, K. R.; Miller, L. L.; Exstrom, C. L. *J. Am. Chem. Soc.* **1998**, *120*, 589. (c) Wong, K. H.; Chan, M. C. W.; Che, C. M. *Chem. Eur. J.* **1999**, *5*, 2845.
(5) Maestri, M.; Sandrini, D.; Balzani, V.; von Zelewsky, A.; Jolliet, P. *Helv. Chim. Acta* **1988**, *71*, 134.
(6) (a) Schwarz, R.; Gliemann, G.; Jolliet, P.; von Zelewsky, A. *Inorg. Chem.* **1989**, *28*, 742. (b) Glasbeek, M.; Sitters, R.; van Veldhoven, E.; von Zelewsky, A.; Humbs, W.; Yersin, H. *Inorg. Chem.* **1998**, *37*, 5159.
(7) García-Herbosa, G.; Muñoz, A.; Maestri, M. *J. Photochem. Photobiol. A: Chem.* **1994**, *83*, 165.
(8) (a) Maestri, M.; Sandrini, D.; Balzani, V.; von Zelewsky, A.; Cornioley-Deuschel, C.; Jolliet, P. *Helv. Chim. Acta* **1988**, *71*, 1053. (b) Barigelletti, F.; Sandrini, D.; Maestri, M.; Balzani, V.; von Zelewsky, A.; Chassot, L.; Jolliet, P.; Maeder, U. *Inorg. Chem.* **1988**, *27*, 3644. (c) Maestri, M.; Cornioley-Deuschel, C.; von Zelewsky, A. *Coord. Chem. Rev.* **1991**, *111*, 117. (d) Jolliet, P.; Gianini, M.; von Zelewsky, A.; Bernardinelli, G.; Stoeckli-Evans, H. *Inorg. Chem.* **1996**, *35*, 4883, and references therein.
(9) Van Houten, K. A.; Heath, D. C.; Barringer, C. A.; Rheingold, A. L.; Pilato, R. S. *Inorg. Chem.* **1998**, *37*, 4647.
(10) Newkome, G. R.; Onishi, M.; Puckett, W. E.; Deutsch, W. A. *J. Am. Chem. Soc.* **1980**, *102*, 4551.
(11) (a) Suggs, J. W.; Dube, M. J.; Nichols, M. *J. Chem. Soc., Chem Commun.* **1993**, 307. (b) Suggs, J. W.; Higgins, J. D., III; Wagner, R. W.; Millard, J. T. In *Metal-DNA Chemistry*, ACS Symposium Series 402; Tullius, T. D., Ed.; American Chemical Society: Washington DC, 1989; p 146.
(12) (a) Tse, M. C.; Cheung, K. K.; Chan, M. C. W.; Che, C. M. *Chem. Commun.* **1998**, 2295. (b) Lai, S. W.; Chan, M. C. W.; Cheung, K. K.; Che, C. M. *Organometallics* **1999**, *18*, 3327.

10.1021/ic991089g CCC: $19.00
Published on Web 12/29/1999

metal−metal and ligand−ligand interactions in these systems and offered insight into their excited-state properties.

Experimental Section

General Procedures. K_2PdCl_4 (Strem), bis(diphenylphosphino)-methane, and 1,5-bis(diphenylphosphino)pentane (dppm and $dppC_5$, respectively; Aldrich) were used as received. 6-Phenyl-2,2′-bipyridine and its derivatives were prepared by literature methods.[13] (**Caution!** *perchlorate salts are potentially explosive and should be handled with care and in small amounts.*) Details of solvent treatment for photophysical studies, instrumentation, and emission measurements have been provided previously.[1]

Syntheses. [Pd(L^{1-5})Cl] (1a−5a, HL^{1-5} = 4-(aryl)-6-phenyl-2,2′-bipyridine; aryl = H (1), phenyl (2), 4-chlorophenyl (3), 4-tolyl (4), 4-methoxyphenyl (5)). A modification of Constable's method was used.[14] A mixture of K_2PdCl_4 (0.16 g, 0.49 mmol) and HL^{1-5} (except L^3, 0.49 mmol) in CH_3CN/H_2O (15/15 mL) was refluxed for 18 h to give a yellow suspension, which was then evaporated to dryness. The product was extracted with dichloromethane, and the volume of extract was reduced to ∼5 mL. Addition of diethyl ether yielded a yellow solid, which was recrystallized by vapor diffusion of diethyl ether into an acetonitrile solution to afford a yellow crystalline solid.

1a. Yield: 0.16 g, 87%. Anal. Calcd for $C_{16}H_{11}N_2PdCl$: C, 51.50; H, 2.97; N, 7.51. Found: C, 51.60; H, 2.85; N, 7.50. MS (+ve FAB): *m*/*z* 372 (M^+), 337 (M^+ − Cl). ^1H NMR (DMSO-d_6): δ 7.09 (m, 2H), 7.52 (d, 1H, *J* = 7.1 Hz), 7.62 (d, 1H, *J* = 7.2 Hz), 7.78 (m, 1H), 7.99 (d, 1H, *J* = 7.9 Hz), 8.14 (t, 1H, *J* = 7.9 Hz), 8.20 (d, 1H, *J* = 7.9 Hz), 8.24 (t, 1H, *J* = 7.8 Hz), 8.48 (d, 1H, *J* = 8.0 Hz), 8.63 (d, 1H, *J* = 4.7 Hz). $^{13}C\{^1H\}$ NMR (DMSO-d_6): δ 119.7, 119.8, 123.1, 124.5, 124.7, 127.4, 129.6, 136.1, 140.1, 140.4, 148.0, 149.0, 153.5, 154.0, 155.1, 163.6.

2a. Yield: 0.19 g, 85%. Anal. Calcd for $C_{22}H_{15}N_2PdCl$: C, 58.82; H, 3.37; N, 6.24. Found: C, 59.05; H, 3.25; N, 6.32. MS (+ve FAB): *m*/*z* 448 (M^+). ^1H NMR (CD_3CN): δ 7.12 (m, 2H), 7.59−7.66 (m, 5H), 7.94 (m, 2H), 8.00 (m, 1H), 8.15 (m, 2H), 8.33 (d, 1H, *J* = 7.9 Hz), 8.73 (m, 2H). $^{13}C\{^1H\}$ NMR (DMSO-d_6): δ 117.9, 118.3, 124.4, 125.6, 125.9, 128.4, 128.5, 130.0, 130.5, 131.3, 137.0, 141.2, 149.0, 149.9, 152.0, 154.8, 155.0, 156.2, 164.7.

3a. A mixture of K_2PdCl_4 (0.16 g, 0.49 mmol) in H_2O (10 mL) and HL^3 (0.17 g, 0.50 mmol) in CH_3CN (40 mL) was refluxed for 30 h to yield an orange suspension, which was filtered and washed with water (3 × 20 mL) and diethyl ether (3 × 20 mL). Extraction using dimethylformamide (DMF) and recrystallization by diffusion of diethyl ether into a DMF solution gave a yellow solid. Yield: 0.16 g, 67%. Anal. Calcd for $C_{22}H_{14}N_2PdCl_2$: C, 54.63; H, 2.92; N, 5.79. Found: C, 54.90; H, 3.10; N, 5.95. MS (+ve FAB): *m*/*z* 482 (M^+). ^1H NMR (DMSO-d_6): δ 7.03−7.12 (m, 2H), 7.52 (br d, 1H, *J* = 6.7 Hz), 7.68 (d, 2H, *J* = 8.6 Hz), 7.76−7.84 (m, 2H), 8.16 (d, 2H, *J* = 8.6 Hz), 8.24−8.31 (m, 2H), 8.54 (s, 1H), 8.63 (br d, 1H, *J* = 4.3 Hz), 8.72 (d, 1H, *J* = 8.0 Hz). $^{13}C\{^1H\}$ NMR (DMSO-d_6): δ 116.9, 117.2, 123.5, 124.5, 125.0, 127.4, 129.0, 129.4, 129.6, 134.8, 135.3, 136.1, 140.2, 148.0, 149.0, 149.6, 153.9, 154.1, 155.2, 163.8.

4a. Yield: 0.17 g, 75%. Anal. Calcd for $C_{23}H_{17}N_2PdCl$: C, 59.63; H, 3.70; N, 6.05. Found: C, 59.70; H, 3.85; N, 6.12. MS (+ve FAB): *m*/*z* 462 (M^+). ^1H NMR (DMSO-d_6): δ 2.42 (s, 3H, Me), 7.09 (m, 2H), 7.42 (d, 2H, *J* = 7.7 Hz), 7.53 (d, 1H, *J* = 6.4 Hz), 7.79−7.86 (m, 2H), 8.04 (d, 2H, *J* = 7.8 Hz), 8.30 (m, 2H), 8.53 (s, 1H), 8.65 (br d, 1H, *J* = 4.2 Hz), 8.74 (d, 1H, *J* = 7.6 Hz). $^{13}C\{^1H\}$ NMR (DMSO-d_6): δ 20.9 (Me), 116.6, 116.9, 123.4, 124.6, 124.8, 127.3, 127.4, 129.5, 129.7, 133.3, 136.2, 140.2, 140.3, 148.2, 149.1, 151.2, 153.9, 154.1, 155.5, 164.0.

5a. Yield 0.18 g, 77%. Anal. Calcd for $C_{23}H_{17}N_2OPdCl$: C, 57.64; H, 3.58; N, 5.84. Found: C, 57.70; H, 3.65; N, 5.90. MS (+ve FAB): *m*/*z* 478 (M^+). ^1H NMR (DMSO-d_6): δ 3.88 (s, 3H, OCH_3), 7.04−7.17 (m, 4H), 7.52 (d, 1H, *J* = 7.0 Hz), 7.76−7.86 (m, 2H), 8.13 (d, 2H, *J* = 8.8 Hz), 8.28 (m, 2H), 8.51 (s, 1H), 8.62 (d, 1H, *J* = 5.1 Hz), 8.74 (d, 1H, *J* = 8.0 Hz). $^{13}C\{^1H\}$ NMR (DMSO-d_6): δ 55.4 (OCH_3), 114.4, 115.9, 116.4, 123.4, 124.5, 124.9, 127.3, 128.0, 129.1, 129.4, 136.0, 140.2, 148.2, 148.9, 150.4, 153.7, 154.1, 155.3, 161.1, 163.6.

[Pd(L^1)Br], 1b. A mixture of **1a** (0.20 g, 0.54 mmol) in CH_3CN (30 mL) and excess NaBr (0.50 g, 4.86 mmol) in CH_3OH (10 mL) was stirred for 24 h at room temperature to afford a yellow solid, which was filtered and washed with water and diethyl ether. Recrystallization by vapor diffusion of diethyl ether into a dimethylformamide solution afforded a yellow crystalline solid. Yield: 0.14 g, 63%. Anal. Calcd for $C_{16}H_{11}N_2PdBr$: C, 46.02; H, 2.66; N, 6.71. Found: C, 46.10; H, 2.70; N, 6.70. MS (+ve FAB): *m*/*z* 417 (M^+). ^1H NMR (DMSO-d_6): δ 7.01−7.11 (m, 2H), 7.63 (d, 1H, *J* = 7.3 Hz), 7.73−7.79 (m, 2H), 8.00 (d, 1H, *J* = 7.4 Hz), 8.13−8.27 (m, 3H), 8.48 (d, 1H, *J* = 8.0 Hz), 8.78 (d, 1H, *J* = 4.7 Hz). $^{13}C\{^1H\}$ NMR (DMSO-d_6): δ 119.8, 119.9, 123.2, 124.6, 124.7, 127.5, 129.9, 138.4, 140.2, 140.3, 148.1, 149.9, 153.5, 153.9, 155.3, 163.4.

[Pd(L^1)I], 1c. The procedure for **1b** was adopted using **1a** (0.20 g, 0.54 mmol) and NaI (0.50 g, 3.34 mmol) to give the product as a yellow crystalline solid. Yield: 0.15 g, 62%. Anal. Calcd for $C_{16}H_{11}N_2PdI$: C, 41.36; H, 2.39; N, 6.03. Found: C, 41.25; H, 2.27; N, 5.90. MS (+ve FAB): *m*/*z* 463 (M^+). ^1H NMR (DMSO-d_6): δ 6.97 (t, 1H, *J* = 7.1 Hz), 7.09 (t, 1H, *J* = 6.9 Hz), 7.67 (d, 1H, *J* = 6.9 Hz), 7.76 (t, 1H, *J* = 6.0 Hz), 8.04 (d, 1H, *J* = 6.9 Hz), 8.12 (d, 1H, *J* = 7.8 Hz), 8.18−8.26 (m, 3H), 8.50 (d, 1H, *J* = 8.0 Hz), 9.03 (d, 1H, *J* = 4.8 Hz). $^{13}C\{^1H\}$ NMR (DMSO-d_6): δ 119.9, 120.0, 123.4, 124.3, 125.0, 127.8, 130.4, 134.9, 140.1, 140.3, 148.4, 151.7, 153.4, 153.6, 155.5, 163.1.

[Pd(L^1)PPh$_3$]ClO$_4$, 1d(ClO$_4$). A mixture of **1a** (0.10 g, 0.27 mmol) and PPh_3 (0.07 g, 0.27 mmol) in CH_3CN/CH_3OH (20/20 mL) was stirred for 3 h at room temperature. Excess $LiClO_4$ (0.20 g, 1.63 mmol) was added to the resultant mixture, which was stirred at room temperature for 5 h and then filtered and concentrated to ∼5 mL. Addition of diethyl ether yielded a yellow solid, which was filtered and washed with diethyl ether. Recrystallization by vapor diffusion of diethyl ether into an acetonitrile solution gave a yellow crystalline solid. Yield: 0.15 g, 80%. Anal. Calcd for $C_{34}H_{26}N_2O_4PdClP$: C, 58.39; H, 3.75; N, 4.01. Found: C, 58.20; H, 3.70; N, 3.95. MS (+ve FAB): *m*/*z* 600 (M^+). ^1H NMR (DMSO-d_6): δ 6.27 (d, 1H, *J* = 5.2 Hz), 6.34 (m, 1H), 6.65 (t, 1H, *J* = 7.3 Hz), 7.05−7.18 (m, 3H), 7.57−7.71 (m, 8H), 7.81−7.93 (m, 6H), 8.12−8.35 (m, 4H), 8.54 (d, 1H, *J* = 8.0 Hz), 8.74 (br s, 1H). $^{13}C\{^1H\}$ NMR (DMSO-d_6): δ 120.4, 120.6, 123.9, 125.9, 126.0, 126.4, 128.3, 128.7, 129.4, 129.9, 132.0, 134.9, 138.2, 138.3, 141.1, 142.4, 149.6, 149.8, 150.2, 152.8, 157.0, 162.2. $^{31}P\{^1H\}$ NMR (CD_3CN): δ 40.38.

[Pd$_2$(L^{1-5})$_2$(μ-dppm)](ClO$_4$)$_2$, 1e-5e(ClO$_4$)$_2$. A mixture of [PdL^{1-5}Cl] (0.32 mmol) and dppm (0.16 mmol) in CH_3CN/CH_3OH (15/15 mL) was stirred for 12 h under a nitrogen atmosphere. Excess $LiClO_4$ was added and the resulting solution was concentrated to ∼5 mL. Addition of diethyl ether afforded a yellow solid, which was filtered and washed with water (3 × 20 mL) and diethyl ether (2 × 20 mL). Recrystallization by vapor diffusion of diethyl ether into an acetonitrile solution afforded yellow crystals.

1e(ClO$_4$)$_2$. Yield: 0.16 g, 79%. Anal. Calcd for $C_{57}H_{44}N_4O_8Pd_2Cl_2P_2$: C, 54.39; H, 3.52; N, 4.45. Found: C, 54.52; H, 3.38; N, 4.32. MS (+ve FAB): *m*/*z* 1157 (M^+ + ClO_4). ^1H NMR (CD_3CN): δ 4.60 (t, 2H, ^2J(PH) = 12.6 Hz, PCH_2P), 6.02 (d, 2H, *J* = 5.2 Hz), 6.28 (t, 2H, *J* = 7.4 Hz), 6.48 (t, 2H, *J* = 7.4 Hz), 6.68−6.75 (m, 4H), 6.98 (d, 2H, *J* = 7.7 Hz), 7.39−7.47 (m, 10H), 7.55−7.59 (m, 4H), 7.75−7.98 (m, 16H). $^{13}C\{^1H\}$ NMR (CD_3CN): δ 21.3 (t, ^1J(PC) = 22 Hz, PCH_2P), 121.0, 124.1, 127.2, 127.8, 130.4, 131.1, 133.2, 134.5, 139.9, 140.9, 143.0, 150.0, 151.5, 152.3, 153.7, 157.1, 163.2. $^{31}P\{^1H\}$ NMR (CD_3CN): δ 35.95.

2e(ClO$_4$)$_2$. Yield: 0.18 g, 78%. Anal. Calcd for $C_{69}H_{52}N_4O_8Pd_2Cl_2P_2$: C, 58.74; H, 3.71; N, 3.97. Found: C, 58.50; H, 3.65; N, 3.92. MS (+ve FAB): *m*/*z* 1311 (M^+ + ClO_4). ^1H NMR (CD_3CN): δ 4.63 (t, 2H, ^2J(PH) = 12.7 Hz, PCH_2P), 6.07 (d, 2H, *J* = 5.2 Hz), 6.31 (t, 2H, *J* = 7.2 Hz), 6.49 (t, 2H, *J* = 7.5 Hz), 6.74−6.81 (m, 4H), 7.19 (d, 2H, *J* = 7.1 Hz), 7.37−7.61 (m, 26 H), 7.86 (t, 4H, *J* = 7.9 Hz), 7.94 (s, 2H), 8.12 (d, 6H, *J* = 8.0 Hz). $^{13}C\{^1H\}$ NMR (CD_3CN): δ 18.9 (t, ^1J(PC) = 22 Hz, PCH_2P), 121.5, 124.6, 124.7, 125.1, 125.8,

(13) Kröhnke, F. *Synthesis* **1976**, 1.
(14) Constable, E. C.; Henney, R. P. G.; Leese, T. A.; Tocher, D. A. *J. Chem. Soc. Chem. Commun.* **1990**, 513.

Table 1. Crystal Data

	1d(ClO_4)	**1e**$(ClO_4)_2$·DMF	**2e**$(ClO_4)_2$
formula	$C_{34}H_{26}N_2O_4PdClP$	$C_{57}H_{44}N_4O_8Pd_2Cl_2P_2$·$(CH_3)_2NCHO$	$C_{69}H_{52}N_4O_8Pd_2Cl_2P_2$
fw	699.44	1331.78	1410.83
crystal system	monoclinic	monoclinic	monoclinic
space group	$P2_1/c$	$P2_1/c$	$P2_1/c$
color	yellow	yellow	yellow
crystal size, mm	0.15 × 0.25× 0.30	0.05 × 0.25 × 0.25	0.30 × 0.30 × 0.45
a, Å	9.801(1)	15.602(2)	14.331(3)
b, Å	20.122(1)	13.253(3)	14.535(3)
c, Å	15.205(1)	27.213(3)	31.901(8)
β, deg	98.096(9)	98.70(2)	93.55(4)
V, Å^3	2968.5(5)	5562(1)	6632(3)
Z	4	4	4
D_c, g cm^{-3}	1.565	1.590	1.413
μ, cm^{-1}	8.12	8.64	7.09
F(000)	1416	2696	2849
$2\theta_{max}$, deg	50	48	45
R,[a] R_w[b]	0.040, 0.056	0.071, 0.087	0.065, 0.084
residual ρ, e Å^{-3}	−0.42, +1.02	−0.73, +1.18	−1.12, +1.05

[a] $R = \sum||F_o| - |F_c||/\sum|F_o|$. [b] $R_w = [\sum w(|F_o| - |F_c|)^2/\sum w|F_o|^2]^{1/2}$.

127.6, 128.5, 129.1, 129.5, 129.8, 130.5, 133.9, 137.2, 138.1, 147.3, 148.9, 149.6, 151.3, 151.8, 154.4, 160.7. $^{31}P\{^1H\}$ NMR (CD_3CN): δ 36.66.

3e(ClO$_4$)$_2$. Yield: 0.15 g, 65%. Anal. Calcd for $C_{69}H_{50}N_4O_8Pd_2Cl_4P_2$: C, 56.01; H, 3.41; N, 3.79. Found: C, 55.88; H, 3.28; N, 3.65. MS (+ve FAB): *m*/*z* 1380 ($M^+ + ClO_4$). ^1H NMR (CD_3CN): δ 4.61 (t, 2H, ^2J(PH) = 12.7 Hz, PCH_2P), 6.02 (m, 2H), 6.28 (m, 2H), 6.40 (t, 2H, *J* = 7.4 Hz), 6.79 (m, 4H), 7.21 (d, 2H, *J* = 7.6 Hz), 7.33−8.22 (m, 36H). $^{13}C\{^1H\}$ NMR (CD_3CN): δ 21.2 (t, ^1J(PC) = 22 Hz, PCH_2P), 116.7, 123.3, 126.3, 126.5, 126.9, 129.0, 129.3, 129.4, 130.4, 130.9, 131.2, 131.6, 132.3, 134.0, 136.8, 138.9, 139.8, 148.9, 150.4, 151.3, 152.0, 153.1, 156.2, 162.6. $^{31}P\{^1H\}$ NMR (CD_3CN): δ 36.64.

4e(ClO$_4$)$_2$. Yield: 0.16 g, 70%. Anal. Calcd for $C_{71}H_{56}N_4O_8Pd_2Cl_2P_2$: C, 59.26; H, 3.92; N, 3.89. Found: C, 59.20; H, 3.85; N, 3.73. MS (+ve FAB): 1339 ($M^+ + ClO_4$). ^1H NMR (CD_3CN): δ 2.42 (s, 6H, Me), 4.61 (t, 2H, ^2J(PH) = 12.7 Hz, PCH_2P), 6.04 (d, 2H, *J* = 5.0 Hz), 6.30 (t, 2H, *J* = 6.9 Hz), 6.45 (t, 2H, *J* = 7.3 Hz), 6.73−6.80 (m, 4H), 7.18 (d, 6H, *J* = 7.8 Hz), 7.47−7.55 (m, 20H), 7.82−7.91 (m, 6H), 8.10 (d, 6H, *J* = 8.0 Hz). $^{13}C\{^1H\}$ NMR (CD_3CN): δ 20.6 (Me), 20.9 (t, ^1J(PC) = 22 Hz, PCH_2P), 116.4, 123.2, 126.2, 126.4, 126.8, 127.3, 129.4, 129.8, 130.1, 131.0, 131.3, 131.6, 132.2, 132.4, 138.8, 139.7, 141.4, 149.0, 150.5, 151.2, 152.9, 153.1, 156.2, 162.3. $^{31}P\{^1H\}$ NMR (CD_3CN): δ 36.53.

5e(ClO$_4$)$_2$. Yield: 0.17 g, 73%. Anal. Calcd for $C_{71}H_{56}N_4O_{10}Pd_2Cl_2P_2$: C, 57.98; H, 3.84; N, 3.81. Found: C, 57.85; H, 3.75; N, 3.90. MS (+ve FAB): *m*/*z* 1369 ($M^+ + ClO_4$). ^1H NMR (CD_3CN): δ 3.88 (s, 6H, OMe), 4.59 (t, 2H, ^2J(PH) = 12.7 Hz, PCH_2P), 6.04 (d, 2H, *J* = 5.2 Hz), 6.28 (t, 2H, *J* = 7.6 Hz), 6.43 (t, 2H, *J* = 7.4 Hz), 6.73−6.80 (m, 4H), 6.87 (d, 4H, *J* = 8.8 Hz), 7.18 (d, 2H, *J* = 7.7 Hz), 7.46−7.60 (m, 20H), 7.78−7.89 (m, 6H), 8.11 (m, 6H). $^{13}C\{^1H\}$ NMR (CD_3CN): δ 22.1 (t, ^1J(PC) = 22 Hz, PCH_2P), 56.3 (OMe), 115.6, 117.0, 117.7, 124.1, 127.1, 127.3, 127.8, 128.5, 130.0, 130.4, 131.1, 139.8, 140.7, 150.2, 151.5, 152.3, 153.9, 157.4, 163.0, 163.3. $^{31}P\{^1H\}$ NMR (CD_3CN): δ 36.29.

[Pd$_2$(L^1)$_2$(μ-dppC$_5$)](ClO$_4$)$_2$, 1f(ClO$_4$)$_2$. The procedure for **1e** was adopted using **1a** (0.15 g, 0.40 mmol) and 1,5-bis(diphenylphosphino)-pentane (0.09 g, 0.20 mmol) to yield a yellow crystalline solid. Yield: 0.19 g, 72%. Anal. Calcd for $C_{61}H_{52}N_4O_8Pd_2Cl_2P_2$: C, 55.72; H, 3.99; N, 4.26. Found: C, 55.68; H, 3.92; N, 4.20. MS (+ve FAB): *m*/*z* 1215 ($M^+ + ClO_4$). ^1H NMR (DMSO-d_6): δ 1.74; 1.83; 2.70 (br m, 10H, $P(CH_2)_5P$), 6.45 (m, 2H), 6.67 (m, 4H), 6.97 (t, 2H, *J* = 7.5 Hz), 7.14 (t, 2H, *J* = 7.0 Hz), 7.46 (m, 8H), 7.55 (m, 4H), 7.67 (d, 2H, *J* = 7.2 Hz), 7.76 (m, 8H), 8.06 (m, 4H), 8.19−8.24 (m, 4H), 8.41 (d, 2H, *J* = 8.0 Hz). $^{13}C\{^1H\}$ NMR (DMSO-d_6): δ 22.6 (d, *J*(PC) = 30 Hz, PCH_2), 24.3 (d, *J*(PC) = 4 Hz, PCH_2CH_2), 30.3 (t, *J*(PC) = 16 Hz, $P(CH_2)_2CH_2$), 119.2, 119.3, 122.7, 124.8, 125.6, 128.1, 128.7, 129.1, 129.2, 130.5, 132.0, 136.0, 136.1, 139.9, 141.1, 148.2, 149.5, 149.6, 151.6, 155.6, 160.9. $^{31}P\{^1H\}$ NMR (CD_3CN): δ 31.51.

X-ray Crystallography. Crystals of **1d**(ClO_4), **1e**$(ClO_4)_2$·DMF, and **2e**$(ClO_4)_2$ were obtained by vapor diffusion of diethyl ether into acetonitrile/dimethylformamide (DMF) solutions. Crystal data and details of collection and refinement are summarized in Table 1. The following data are listed in the order **1d**(ClO_4)/**1e**$(ClO_4)_2$·DMF. A total of 5408/9147 unique reflections was collected at 301 K on a Rigaku/Nonius diffractometer [λ(Mo-Kα) = 0.7107 Å, $\omega-2\theta$ scans]. The structures were solved by Patterson methods, expanded using Fourier techniques (PATTY[15]), and refined by full-matrix least squares using the TeXsan[16] software package for 4180/5692 absorption-corrected (transmission 0.88−1.00/0.83−1.00) reflections with $I > 3\sigma(I)$ and 388/689 parameters. For **2e**$(ClO_4)_2$, a total of 8647 unique reflections was collected at 298 K on a Nonius diffractometer [λ(Mo-Kα) = 0.7107 Å, $\theta/2\theta$ scans]. The structure was solved by Patterson methods, expanded using Fourier techniques, and refined by least-squares treatment on F^2 using the NRCVAX program for 4698 absorption-corrected (transmission 0.65−1.00) reflections with $I > 2\sigma(I)$ and 793 parameters. The pairs of atoms N(1)/C(1) for **1d**(ClO_4), N(1)/C(1) and N(3)/C(17) for **1e**$(ClO_4)_2$·DMF, and N(1)/C(22) and N(3)/C(44) for **2e**$(ClO_4)_2$ were differentiated by their temperature factors; interchanging the respective C and N atoms resulted in unreasonable temperature factors and/or higher *R* values.

Results and Discussion

Synthesis and Characterization. The complexes described in this study are illustrated in Figure 1. Cyclopalladation of the ligands HL^{1-5}, prepared by Kröhnke syntheses,[13] is accomplished by modifying the procedure described by Constable and co-workers.[14] The various 4-aryl substituents in HL^{1-5} may be expected to impose different electronic demands upon the palladium center. Hence complexes **1a**−**5a** are synthesized by interaction of K_2PdCl_4 with HL^{1-5} respectively at elevated temperatures in an acetonitrile/water mixture. The coordinated chloride auxiliary in this series allows derivatization of the $[Pd(L^{1-5})]$ moieties through ligand-substitution reactions. The neutral complexes $[Pd(L^1)X]$ (X = Br, **1b**; I, **1c**) and the cationic derivative $[Pd(L^1)PPh_3]^+$ (**1d**) are formed by reaction of **1a** with NaX and triphenylphosphine respectively at room temperature.

The binuclear cyclometalated Pd(II) complexes **1e**−**5e** and **1f** are conveniently prepared by treatment of the respective

(15) PATTY: Beurskens, P. T.; Admiraal, G.; Beursken, G.; Bosman, W. P.; Garcia-Granda, S.; Gould, R. O.; Smits, J. M. M.; Smykalla, C. The DIRDIF program system, Technical Report of the Crystallography Laboratory, University of Nijmegen, The Netherlands, 1992.
(16) TeXsan: *Crystal Structure Analysis Package*; Molecular Structure Corporation: The Woodlands, TX, 1985 and 1992.

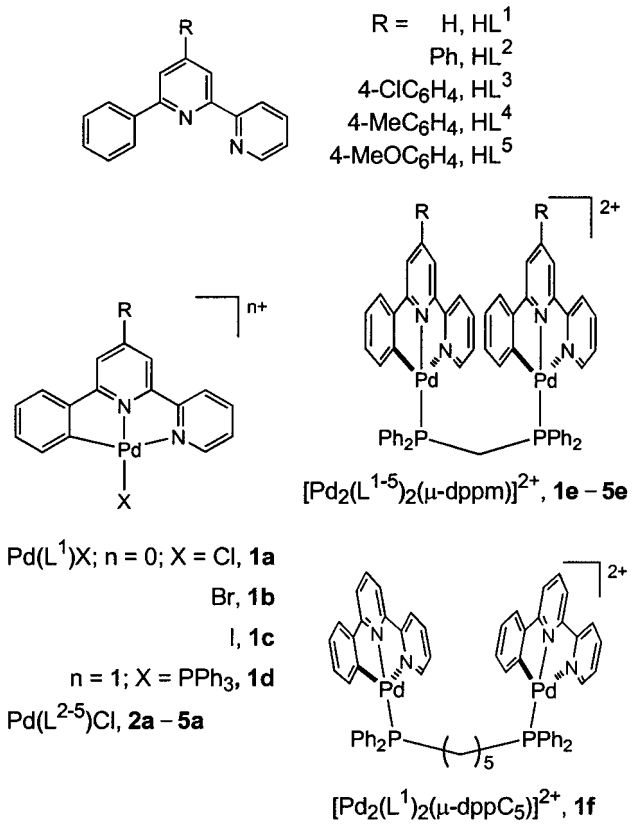

Figure 1. Nomenclature for ligands and complexes.

mononuclear precursor with the appropriate diphosphine ligand. In the ^{1}H NMR spectra, the methylene group of the dppm bridge appears as a distinctive triplet resonance at ca. 4.6 ppm (^2J(PH) = 12.7 Hz). The positive FAB mass spectra for **1e**−**5e** contain a prominent signal corresponding to the ($M^+ + ClO_4$) fragment rather than the molecular cation M^+.

Crystal Structures: Pd−Pd and $\pi-\pi$ Separations. A number of palladium(II) complexes have been crystallographically characterized during this investigation. Comparisons with the structures of platinum(II) congeners can provide insight into the extent of metal−metal and ligand−ligand interactions in these systems. Selected bond distances and angles for **1d**(ClO_4), **1e**$(ClO_4)_2$·DMF, and **2e**$(ClO_4)_2$ are listed in Table 2. Constable and co-workers[14] have communicated the crystal structure of **1a**.

The Pd atom in the cation **1d** (Figure 2) resides in a highly distorted square planar environment. The bite angle of 157.6(2)° exhibited by L^1 is typical for cyclometalating 6-phenyl-2,2′-bipyridine ligands. The palladium−ligand distances are comparable to those in the platinum analogue[2] (e.g., Pd−P, 2.273(1) Å; Pt−P, 2.243(3) Å). In the crystal lattice of **1d**, distinct $\pi-\pi$ stacking interactions are not apparent due to poor overlap of L^1 ligands, although some close intermolecular contacts (3.5−3.7 Å) are observed. This is in contrast to the structure of [Pt(L^1)PPh_3]ClO_4,[2] which displays head-to-tail π-stacking interactions with intermolecular plane separations of 3.35 Å. In addition, Jeffrey, Ward, and co-workers[17] have reported the crystal structure of the Pd(II) complex [Pd(L′)Cl] (HL′ = 6-(2-hydroxyphenyl)-2,2′-bipyridine), which reveals an average stacking distance of 3.44 Å between the L′ planes.

Like the platinum equivalent $[Pt_2(L^1)_2(\mu\text{-dppm})]^{2+}$,[2] the molecular structures of the cations $[Pd_2(L^1)_2(\mu\text{-dppm})]^{2+}$ (**1e**) and $[Pd_2(L^2)_2(\mu\text{-dppm})]^{2+}$ (**2e**) (Figures 3 and 4 respectively) depict two [Pd(L^n)] moieties tethered by a dppm linker. The intramolecular Pd−Pd separations of 3.230(1) Å in **1e** and 3.320(2) Å in **2e** are significantly greater than that expected for a strong Pd−Pd bonding interaction (typically 2.6−2.8 Å).[18] Outside this range, longer Pd−Pd distances have been observed in $[Pd_2(\mu_{NS},\eta^2\text{-L})_2Cl_2(PMe_3)_2]$ (L = heterocyclic 2-thiolate, 2.915(1)−3.104(2) Å),[19] $[Pd_2(C_6H_4N(H)N{=}C(CH_3)C_5H_4N)_2(\mu$-

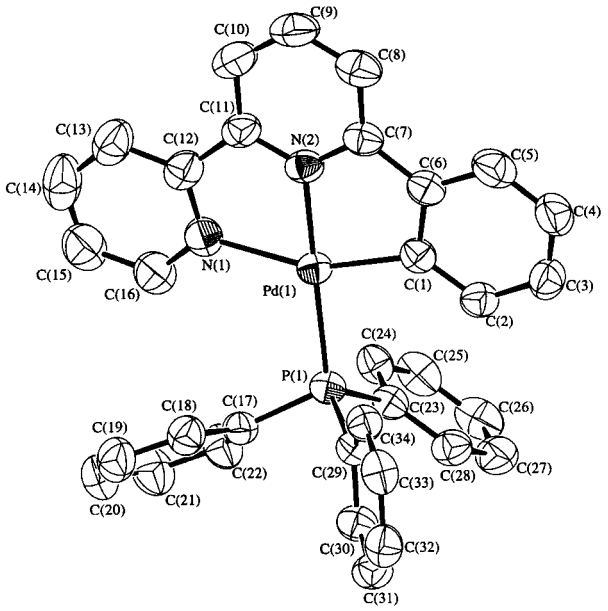

Figure 2. Perspective view of [Pd(L^1)PPh_3]$^+$, **1d** (50% probability ellipsoids).

Table 2. Selected Bond Lengths (Å) and Angles (deg)

[Pd(L^1)PPh_3]ClO_4, **1d**(ClO_4)			
Pd(1)−P(1)	2.273(1)	Pd(1)−N(2)	2.020(4)
Pd(1)−N(1)	2.191(4)	Pd(1)−C(1)	2.039(5)
P(1)−Pd(1)-N(1)	106.7(1)	P(1)−Pd(1)-C(1)	95.6(1)
P(1)−Pd(1)-N(2)	172.8(1)	N(1)−Pd(1)-C(1)	157.6(2)
[$Pd_2(L^1)_2$(μ-dppm)]$(ClO_4)_2$·DMF, **1e**$(ClO_4)_2$·DMF			
Pd(1)−P(1)	2.266(2)	Pd(2)−P(2)	2.272(2)
Pd(1)−N(1)	2.116(9)	Pd(2)−N(3)	2.17(1)
Pd(1)−N(2)	2.025(8)	Pd(2)−N(4)	2.055(8)
Pd(1)−C(1)	2.17(1)	Pd(2)−C(17)	2.07(1)
P(1)−C(45)	1.845(9)	P(2)−C(45)	1.829(9)
P(1)−Pd(1)-N(1)	102.6(3)	P(2)−Pd(2)-N(3)	105.6(3)
P(1)−Pd(1)-N(2)	174.9(3)	P(2)−Pd(2)-N(4)	174.9(2)
P(1)−Pd(1)-C(1)	97.4(3)	P(2)−Pd(2)-C(17)	97.4(3)
N(1)−Pd(1)-C(1)	160.0(4)	N(3)−Pd(2)-C(17)	156.9(4)
Pd(1)−P(1)-C(45)	115.5(3)	Pd(2)−P(2)-C(45)	115.9(3)
P(1)−C(45)-P(2)	122.8(5)		
[$Pd_2(L^2)_2$(μ-dppm)]$(ClO_4)_2$, **2e**$(ClO_4)_2$			
Pd(1)−P(1)	2.279(5)	Pd(2)−P(2)	2.280(5)
Pd(1)−N(1)	2.182(13)	Pd(2)−N(3)	2.177(13)
Pd(1)−N(2)	2.003(12)	Pd(2)−N(4)	1.991(13)
Pd(1)−C(22)	2.021(16)	Pd(2)−C(44)	1.999(17)
P(1)−C(45)	1.853(17)	P(2)−C(45)	1.856(17)
P(1)−Pd(1)-N(1)	105.2(4)	P(2)−Pd(2)-N(3)	106.7(4)
P(1)−Pd(1)-N(2)	175.6(4)	P(2)−Pd(2)-N(4)	175.7(4)
P(1)−Pd(1)-C(22)	96.8(5)	P(2)−Pd(2)-C(44)	95.2(5)
N(1)−Pd(1)-C(22)	157.6(6)	N(3)−Pd(2)-C(44)	157.0(6)
Pd(1)−P(1)-C(45)	116.1(5)	Pd(2)−P(2)-C(45)	117.1(5)
P(1)−C(45)-P(2)	120.5(9)		

(17) Bardwell, D. A.; Crossley, J. G.; Jeffery, J. C.; Orpen, A. G.; Psillakis, E.; Tilley, E. E. M.; Ward, M. D. *Polyhedron*, **1994**, *13*, 2291.

(18) For example, see: (a) Cotton, F. A.; Matusz, M.; Poli, R.; Feng, X. *J. Am. Chem. Soc.* **1988**, *110*, 1144. (b) Ogoshi, S.; Tsutsumi, K.; Ooi, M.; Kurosawa, H. *J. Am. Chem. Soc.* **1995**, *117*, 10415. (c) Tanase, T.; Ukaji, H.; Yamamoto, Y. *J. Chem. Soc., Dalton Trans.* **1996**, 3059.

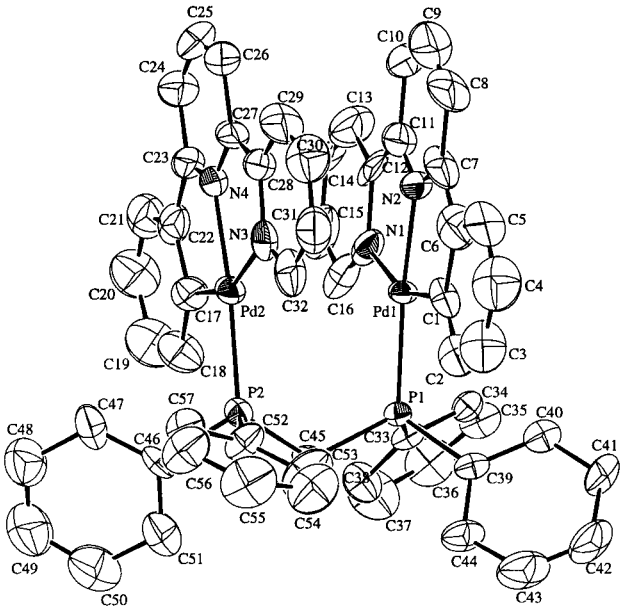

Figure 3. Perspective view of $[Pd_2(L^1)_2(\mu\text{-dppm})]^{2+}$, **1e** (35% probability ellipsoids).

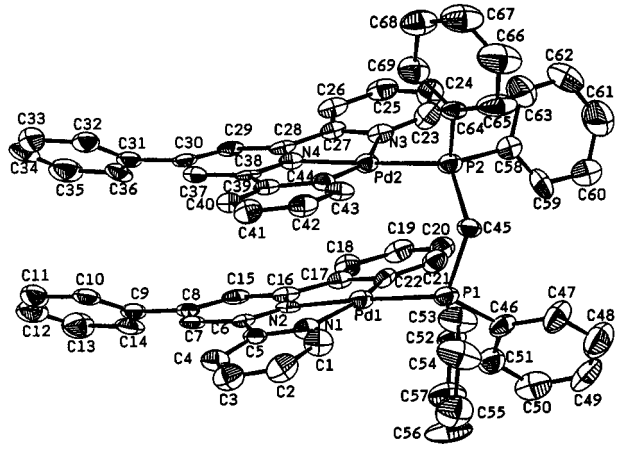

Figure 4. Perspective view of $[Pd_2(L^2)_2(\mu\text{-dppm})]^{2+}$, **2e** (30% probability ellipsoids).

dppm)$](BF_4)_2$ (3.114(1) Å),[20] $[Pd_2(2\text{-}(5'\text{-}MeC_6H_3)\text{-}1,10\text{-phen})_2(\mu\text{-N-3,N-9-adenine})](NO_3)$ (3.162(3) Å),[11a] and $[Pd_2(dppm)_2(CN)_4]$ (3.276(1) Å).[21] The intermolecular Pd-Pd contact of 3.354(4) Å in $[Pd(bpy)(CN)_2]$[22] and the Pt−Pt distance of 3.270(1) Å in $[Pt_2(L^1)_2(\mu\text{-dppm})](ClO_4)_2$[2] should also be noted. Since the latter is indicative of weak intermetal communication and the ionic radius of Pt(II) is larger than that for Pd(II), comparable intramolecular metal−metal separations in **1e**, **2e**, and $[Pt_2(L^1)_2(\mu\text{-dppm})]^{2+}$ imply that the degree of ground-state metal−metal interaction is even smaller in the Pd system.

The small dihedral angles between the two $[Pd(L^n)]$ mean planes in **1e** and **2e** (5.7 and 4.8° respectively) demonstrate that the intramolecular $[Pd(L^n)]$ units are nearly coplanar. The average interplanar separation between the L^n ligands in **1e** and **2e** are 3.34 and 3.35 Å, respectively. This feature and the small dihedral angle signify π-stacking interactions within the binuclear complexes, even though there is apparently minimal Pd−Pd communication in the ground state. The torsion angle of 25.8° (defined by N(2)−Pd(1)−Pd(2)−N(4)) between the two $[Pd(L^1)]$ moieties in **1e** is smaller than the corresponding angle of 44.6° in $[Pt_2(L^1)_2(\mu\text{-dppm})](ClO_4)_2$.[1,2] The magnitude of the latter was attributed to optimized $\pi-\pi$ interactions between the aromatic ligands L^1, to avoid repulsive forces arising from eclipsed overlap of π orbitals (i.e. torsion angle ca. 0°).[23] Hence it appears that, like the metal−metal interaction, the $\pi-\pi$ orbital overlap in **1e** is inferior compared to the platinum analogue. The torsion angle between the two $[Pd(L^2)]$ moieties in **2e** is 5.4° (defined by N(2)−Pd(1)−Pd(2)−N(4)). There are no close intermolecular contacts between the aromatic ligands in the crystal lattices of **1e** and **2e** (distance > 4 Å).

Absorption Spectra. The UV−visible absorption spectra of the mono- and binuclear Pd(II) complexes depicted in this work have been obtained. The UV−vis spectral data of **1a**−**5a** and **1b**−**1d** in dichloromethane are listed in Table 3. For example, the absorption spectrum of **1a** is shown in Figure 5. The intense absorptions at λ_{max} = 272, 278, 309, and 326 nm ($\epsilon \sim 10^4$ dm^3 mol^{-1} cm^{-1}) are assigned to intraligand transitions of the cyclometalated ligand, based on similarities with the absorptions of the free ligand HL^1. There is a moderately intense low-energy band tailing from λ_{max} = 360−450 nm with a shoulder at $\lambda \sim$ 390 nm. The ϵ value at 390 nm is 1150 dm^3 mol^{-1} cm^{-1} and we tentatively assign this band to a spin-allowed 4d(Pd) → $\pi^*(L^1)$ (^{1}MLCT) transition. Absorption bands at λ_{max} = 349−400 nm in the related complexes $[Pd(C,N)_2]$ (HC,N = 2-phenylpyridine, 2-(2′-thienyl)pyridine, 7,8-benzoquinoline) have also been ascribed to MLCT transitions,[5] and the red shift of similar bands in analogous Pt(II) derivatives provides support for this assignment (see below). The MLCT transition of the cationic derivative [Pd(terpy)Cl][PF_6] was previously assigned at λ_{max} = 328−362 nm.[24] Ligand-field d−d transitions have been invoked for absorptions in the 380−400 nm range for orthometalated azobenzene Pd(II) complexes,[25] but unreasonably high ϵ values (ca. 8×10^3 dm^3 mol^{-1} cm^{-1}) are reported. We reason that the ϵ value at 390 nm for **1a** is also larger than would be expected for d−d transitions in Pd(II) derivatives. Similar assignments can be made for complexes **1b**, **1c**, and **2a**−**5a**: the absorptions at $\lambda_{max} \leq$ 370 nm are assigned as intraligand in nature while the low-energy bands at $\lambda_{max} \geq$ 390 nm are attributed to MLCT transitions. The low-energy absorption for **1d** is blue-shifted to λ_{max} 375 nm (ϵ = 1950 dm^3 mol^{-1} cm^{-1}) in CH_3CN, and this is consistent with the expected increase in the energy of the MLCT transition for cationic species.

The UV−visible spectral data of complexes **1e**−**5e** and **1f** in acetonitrile are listed in Table 4. The absorption spectrum of $[Pd_2(L^1)_2(\mu\text{-dppm})]^{2+}$ (**1e**) shows intense intraligand transitions at λ_{max} 309 and 331 nm ($\epsilon \sim 10^4$ dm^3 mol^{-1} cm^{-1}) and moderately intense and broad absorptions at λ_{max} 378−401 nm (ϵ = 4900−3400 dm^3 mol^{-1}cm^{-1}) (Figure 6). All the absorption bands obey Beer's law in the concentration range 5×10^{-6} to 5×10^{-3} mol dm^{-3}. By comparison with the mononuclear counterpart **1d**, it is evident that the spectra are very similar, except that the ϵ values are greater for **1e** (Figure 6). This may be rationalized by an increase in the number of Pd(L^1) chromophores per molecule. For d^8 systems, a dσ^* → π^* metal−

(19) Yap, G. P. A.; Jensen, C. M. *Inorg. Chem.* **1992**, *31*, 4823.
(20) García-Herbosa, G.; Muñoz, A.; Miguel, D.; García-Granda, S. *Organometallics* **1994**, *13*, 1775.
(21) Yip, H. K.; Lai, T. F.; Che, C. M. *J. Chem. Soc., Dalton Trans.* **1991**, 1639.
(22) Che, C. M.; He, L. Y.; Poon, C. K.; Mak, T. C. W. *Inorg. Chem.* **1989**, *28*, 3081.
(23) Hunter, C. A.; Sanders, J. K. M. *J. Am. Chem. Soc.* **1990**, *112*, 5525.
(24) Zhang, W.; Bensimon, C.; Crutchley, R. J. *Inorg. Chem.* **1993**, *32*, 5808.
(25) Wakatsuki, Y.; Yamazaki, H.; Grutsch, P. A.; Santhanam, M.; Kutal, C. *J. Am. Chem. Soc.* **1985**, *107*, 8153.

Table 3. UV−Visible Spectral Data of Mononuclear Complexes[a]

complex	λ_{max}/nm (ϵ/dm^3 mol^{-1}cm^{-1})
Pd(L^1)Cl, **1a**	272 (27 300), 278 (27 600), 309 (15 900), 326 (15 900), 342 (sh, 9500), 390 (sh, 1150), 421 (sh, 350)
Pd(L^2)Cl, **2a**	263 (26 700), 287 (40 600), 328 (18 600), 349 (sh, 11 500), 394 (sh, 1600), 422 (sh, 510)
Pd(L^3)Cl, **3a**	266 (25 400), 291 (39 900), 329 (18 600), 350 (sh, 12 000), 401 (sh, 1350), 428 (sh, 370)
Pd(L^4)Cl, **4a**	263 (23 000), 294 (33 400), 329 (18 800), 346 (sh, 13 000), 369 (sh, 5100), 397 (sh, 1500), 422 (450)
Pd(L^5)Cl, **5a**	262 (26 700), 278 (26 300), 312 (34 500), 335 (sh, 25 100), 347 (sh, 20 100), 369 (sh, 11 400), 398 (sh, 2350), 423 (540)
Pd(L^1)Br, **1b**	272 (22 300), 279 (23 000), 311 (15 300), 326 (14 700), 343 (sh, 9000), 395 (sh, 1100), 418 (sh, 410)
Pd(L^1)I, **1c**	249 (28 500), 268 (22 000), 317 (15 800), 328 (15 000), 390 (sh, 2200), 418 (sh, 940)
[Pd(L^1)PPh$_3$](ClO$_4$), **1d**(ClO$_4$)[b]	243 (48 300), 267 (sh, 26 400), 306 (13 000), 331 (sh, 10 400), 375 (1950), 397 (sh, 1250)

[a] In CH_2Cl_2 unless stated otherwise. [b] In acetonitrile.

Table 4. UV−Visible Spectral Data of Binuclear Complexes in Acetonitrile

Complex	λ_{max}/nm (ϵ/dm^3 mol^{-1}cm^{-1})
[Pd$_2$(L^1)$_2$(μ-dppm)](ClO$_4$)$_2$, **1e**(ClO$_4$)$_2$	309 (22 000), 331 (sh, 18 500), 378 (4900), 401 (sh, 3400)
[Pd$_2$(L^2)$_2$(μ-dppm)](ClO$_4$)$_2$, **2e**(ClO$_4$)$_2$	286 (69 800), 311 (sh, 44 400), 386 (4900), 408 (sh, 3200)
[Pd$_2$(L^3)$_2$(μ-dppm)](ClO$_4$)$_2$, **3e**(ClO$_4$)$_2$	288 (71 300), 314 (sh, 51 100), 390 (4800), 412 (sh, 3100)
[Pd$_2$(L^4)$_2$(μ-dppm)](ClO$_4$)$_2$, **4e**(ClO$_4$)$_2$	291 (57 400), 316 (49 500), 387 (4700), 410 (sh, 2700)
[Pd$_2$(L^5)$_2$(μ-dppm)](ClO$_4$)$_2$, **5e**(ClO$_4$)$_2$	303 (46 200), 330 (51 300), 396 (sh, 7100), 418 (sh, 2900)
[Pd$_2$(L^1)$_2$(μ-dppC$_5$)](ClO$_4$)$_2$, **1f**(ClO$_4$)$_2$	307 (25 600), 318 (25 100), 378 (4700), 398 (sh, 3100)

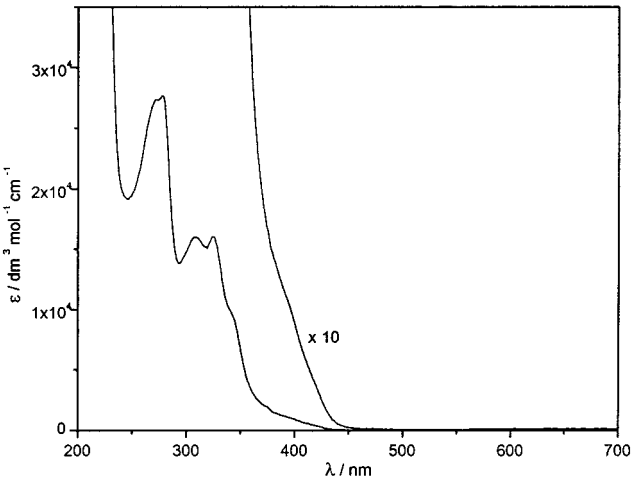

Figure 5. UV−vis absorption spectrum of **1a** in CH_2Cl_2 at 298 K.

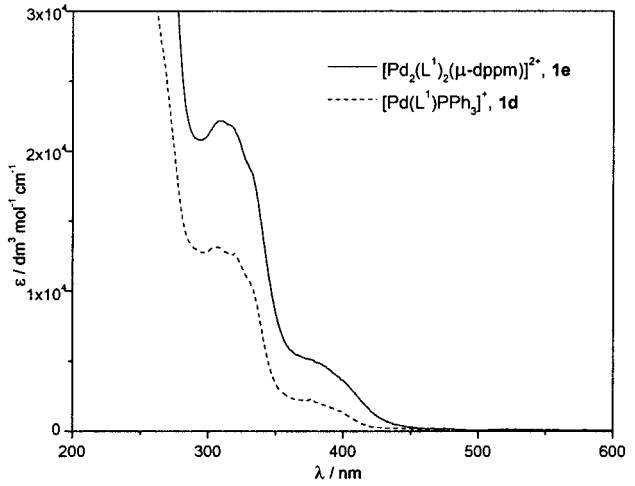

Figure 6. UV−vis absorption spectra of **1d** and **1e** in CH_3CN at 298 K.

metal-to-ligand charge transfer (MMLCT) transition which is red-shifted from the MLCT transition of mononuclear species is expected for binuclear derivatives exhibiting significant metal−metal interaction (Figure 7).[1,26] The virtual match

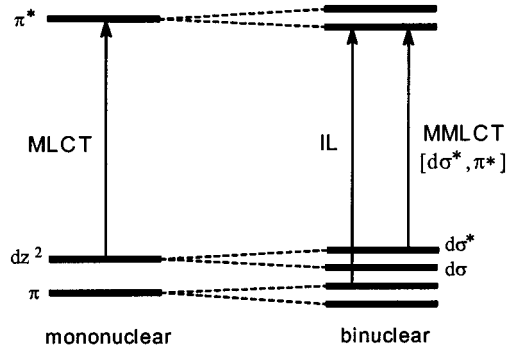

Figure 7. Schematic molecular orbital diagram illustrating metal−metal and ligand−ligand interactions in binuclear polypyridine d^8−d^8 complexes.

between the low-energy absorptions at $\lambda > 360$ nm for **1d** and **1e**, together with the structural parameters (see above), thus imply very weak or minimal Pd−Pd interaction in **1e**. Accordingly, the absorptions at $\lambda_{max} = 378-401$ nm for **1e** are tentatively assigned as MLCT in nature like for **1d**. Furthermore, the low-energy absorption of **1f**, in which [Pd(L^1)] units are separated by a long diphosphine ligand and Pd−Pd communication is disfavored, is almost identical to that for **1e** (Table 4). This observation reinforces the notion that there is minimal ground-state metal−metal interaction in these binuclear Pd(II) complexes. Similar assignments can be made with respect to the absorption spectra of **2e**−**5e**.

Emission Spectra. All complexes in this account are nonemissive at room temperature. At 77 K, the cationic derivatives bearing phosphine ligands generally display more intense emissions than neutral species (Table 5). Indeed, the [Pd(L$^{1-5}$)Cl] (**1a**−**5a**) and [Pd(L^1)X] (X = Br, **1b**; I, **1c**) solids are nonemissive at 298 and 77 K.[27] The cationic complex [Pd(L^1)(PPh$_3$)]$^+$ (**1d**) and the related dication [Pd$_2$(L^1)$_2$(μ-dppC$_5$)]$^{2+}$ (**1f**) display vibronically structured emissions at $\lambda_{max} = 467-576$ and 474−586 nm, respectively, in 77 K glassy MeOH/EtOH solutions, with vibronic progressions of ca. 1300 cm^{-1} (Figure 8) and lifetimes (τ) in the order of 10^{-4} s. These high-energy bands can be assigned to intraligand (^{3}IL) emission by the cyclometalated ligand L^1. The cationic derivatives **1e**−

(26) Miskowski, V. M.; Houlding, V. H. *Inorg. Chem.* **1991**, *30*, 4446.

(27) These complexes are weakly emissive in frozen dichloromethane at 77 K.

Table 5. 77 K Emission Data (complex concentration 1×10^{-4} M)

complex	λ_{max}/nm MeOH/EtOH (1:1)	λ_{max}/nm Solid
$[Pd_2(L^1)_2(\mu\text{-dppm})](ClO_4)_2$, **1e**$(ClO_4)_2$	480, 510, 626	526, 553
$[Pd_2(L^2)_2(\mu\text{-dppm})](ClO_4)_2$, **2e**$(ClO_4)_2$	480, 523, 633	516 (max), 556
$[Pd_2(L^3)_2(\mu\text{-dppm})](ClO_4)_2$, **3e**$(ClO_4)_2$	480, 523, 658	529, 566
$[Pd_2(L^4)_2(\mu\text{-dppm})](ClO_4)_2$, **4e**$(ClO_4)_2$	478, 514, 632	544 (max), 578
$[Pd_2(L^5)_2(\mu\text{-dppm})](ClO_4)_2$, **5e**$(ClO_4)_2$	479 (sh), 517, 634	526 (max), 560
$[Pd_2(L^1)_2(\mu\text{-dppC}_5)](ClO_4)_2$, **1f**$(ClO_4)_2$	474 (max), 507, 542, 586 (sh)	498 (max), 527
$[Pd(L^1)PPh_3](ClO_4)$, **1d**(ClO_4)	467 (max), 501, 532, 576 (sh)	493 (max), 527, 563

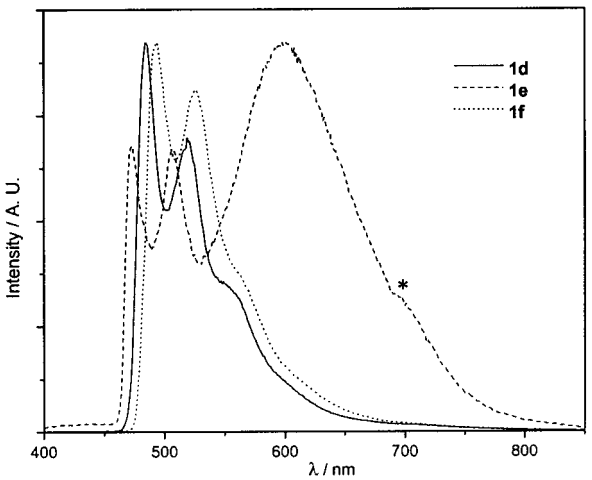

Figure 8. Normalized 77 K emission spectra of **1d**, **1e**, and **1f** in 1:1 MeOH/EtOH glass ($\lambda_{ex} = 350$ nm, * denotes instrumental artifact).

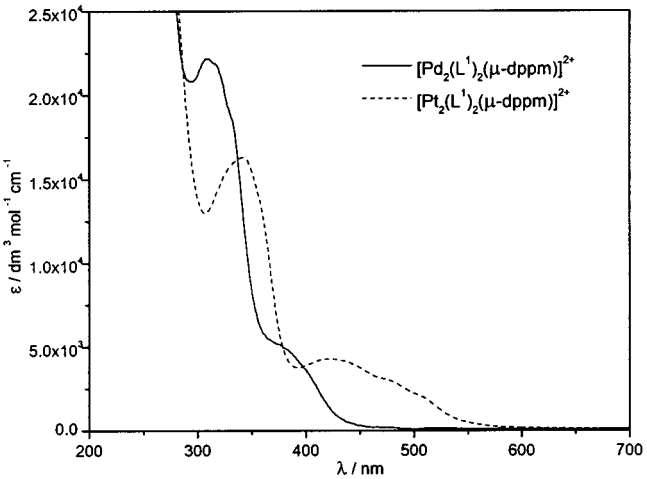

Figure 9. UV−vis absorption spectra of $[M_2(L^1)_2(\mu\text{-dppm})]^{2+}$ (M = Pd, Pt) in CH_3CN at 298 K.

5e$(ClO_4)_2$, **1d**(ClO_4)**,** and **1f**$(ClO_4)_2$ are luminescent in the solid state at 77 K.[28] Except for **1e**$(ClO_4)_2$ and **3e**$(ClO_4)_2$, highly structured emissions at $\lambda_{max} = 493-578$ nm are displayed, and these are ascribed to metal-perturbed ^{3}IL excited states. The solid emissions of **1e**$(ClO_4)_2$ ($\lambda_{max} = 526-553$ nm) and **3e**$(ClO_4)_2$ ($\lambda_{max} = 529-566$ nm) are more diffuse.

Complexes **1e**−**5e** are luminescent in glassy MeOH/EtOH solutions (Table 5). The emission spectrum of **1e** (Figure 8) shows sharp bands at $\lambda_{max} = 480$ and 510 nm ($\tau = 160$ μs, vibronic progression 1225 cm^{-1}) and a broad structureless band at 626 nm ($\tau = 90$ μs). The high-energy structure resembles the intraligand emission of **1d** and **1f** and is therefore assigned to a ^{3}IL excited state. The broad emission at 626 nm is tentatively assigned to an excimeric ^{3}IL transition resulting from $\pi-\pi$ interactions.[29] There are evidently various static conformations for **1e** in glassy alcohol solution, and only some of these can exhibit substantial excimeric character in their lowest ^{3}IL excited states. A d$\sigma^* \rightarrow \pi^*$ MMLCT assignment is not preferred due to the lack of evidence for appreciable Pd−Pd bonding. The absence of a low-energy band for **1d** and **1f** suggests that their geometry disfavor such $\pi-\pi$ interactions. Complexes **2e** and **5e** exhibit dual emissions at $\lambda_{max} = 480$, 523 ($\tau = 64$ μs), and 633 nm ($\tau = 88$ μs) and $\lambda_{max} = 479$ (sh), 517 ($\tau = 74$ μs), and 634 nm ($\tau = 16$ μs), respectively, in MeOH/EtOH glasses. Like the Pt(II) analogues,[1] no apparent photophysical trend arising from the various 4-aryl substituents is observed.

Our investigation has shown that the nature of the luminescent excited states of **1e**−**5e** is highly dependent upon the solvent and medium. For example, their emission spectra in frozen acetonitrile at 77 K contain structureless bands at $\lambda_{max} \sim 600$ nm only (assignable to $\pi-\pi$ excimeric ^{3}IL transitions), and no high-energy vibronic bands are detected as in MeOH/EtOH glasses. Changes in emissive excited states in different solvents have been reported for binuclear Pt(II) terpyridine complexes.[30] The π-stacking conformations leading to an excimeric low-energy emission are apparently facilitated in rigid, frozen solutions; **1e**−**5e**$(ClO_4)_2$ solids do not emit at $\lambda_{max} \geq 600$ nm. This is consistent with the X-ray structural data that revealed non-ideal $\pi-\pi$ interactions in the crystal lattices. The structured solid-state emissions (Table 5) are slightly red-shifted from those of MeOH/EtOH glasses, perhaps due to very weak $\pi-\pi$ interactions.

Comparisons between Pd(II) and Pt(II) Systems. A principal objective of this work is to highlight spectroscopic similarities and differences between the cyclometalated 6-phenyl-2,2′-bipyridine Pd(II) and Pt(II) congeners,[1,2] in order to shed further light upon the nature of their excited states and intramolecular (d^8-d^8 and $\pi-\pi$) interactions.

The absorption at $\lambda \sim 390$ nm for $[Pd(L^1)Cl]$ (**1a**) in CH_2Cl_2 is assigned to a MLCT transition. Since the 4d(Pd) orbital exhibits a higher ionization potential than 5d(Pt), a red shift for the corresponding absorption in $[Pt(L^1)Cl]$ ($\lambda_{max} = 430$ nm in CH_2Cl_2) is consistent with this assignment. Shifting of MLCT transitions to lower energies for [M(bph)(bpy)] (H_2bph = biphenyl) from Pd(II) to Pt(II) has been reported.[31] A compari-

(28) Non-linear exponential decays for solid-state emission lifetimes were observed.

(29) Comparable emissions have been observed for Pt(II) terpyridine complexes: (a) Bailey, J. A.; Hill, M. G.; Marsh, R. E.; Miskowski, V. M.; Schaefer, W. P.; Gray, H. B. *Inorg. Chem.* **1995**, *34*, 4591. (b) Arena, G.; Calogero, G.; Campagna, S.; Scolaro, L. M.; Ricevuto, V.; Romeo, R. *Inorg. Chem.* **1998**, *37*, 2763. (c) Lai, S. W.; Chan, M. C. W.; Cheung, K. K.; Che, C. M. *Inorg. Chem.* **1999**, *38*, 4262.

(30) Bailey, J. A.; Miskowski, V. M.; Gray, H. B. *Inorg. Chem.* **1993**, *32*, 369.

(31) Cornioley-Deuschel, C.; von Zelewsky, A. *Inorg. Chem.* **1987**, *26*, 3354.

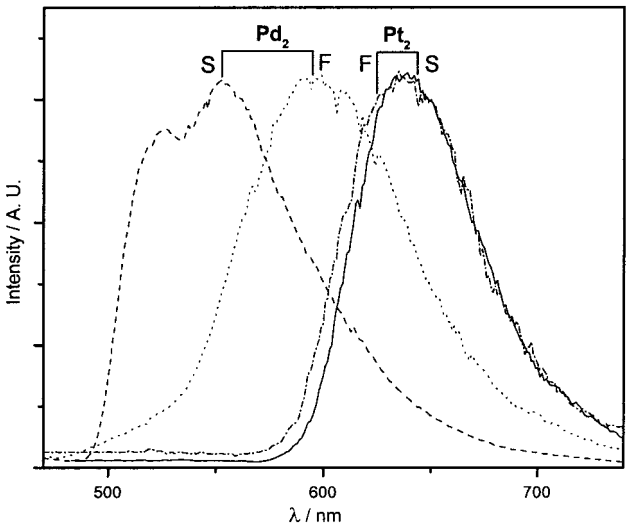

Figure 10. Normalized 77 K emission spectra (λ_{ex} = 350 nm) of $[M_2(L^1)_2(\mu\text{-dppm})](ClO_4)_2$ (M = Pd, Pt) in frozen CH_3CN (F) and solid state (S).

son between the UV absorption spectra of $[Pd_2(L^1)_2(\mu\text{-dppm})]^{2+}$ (**1e**) and its Pt(II) analogue is depicted in Figure 9. The platinum derivative has noticeably higher absorbance at λ_{max} = 450−600 nm, a region where mononuclear counterparts do not absorb, and a d$\sigma^* \rightarrow \pi^*$ transition was previously assigned. We again conclude that the apparent blue shift in the lowest energy band for **1e** signifies exceedingly weak/minimal Pd−Pd interaction in the ground state.

Correlation of luminescent properties between the Pd(II) and Pt(II) counterparts is also informative. The 77 K emission of $[M_2(L^1)_2(\mu\text{-dppm})]^{2+}$ in frozen CH_3CN occurs at λ_{max} = 598 and 638 nm for Pd and Pt, respectively (Figure 10). Since a $\pi-\pi$ excimeric ^{3}IL transition is invoked for the Pd_2 species, the red shift for the Pt_2 analogue is indicative of an excited-state arising from $\pi-\pi$ (excimeric ^{3}IL) *and* metal−metal (previously assigned as d$\sigma^* \rightarrow \pi^*$) interactions. In other words, the Pd−Pd interaction in the excited state appears weaker. The 77 K solid-state emission spectra for $[M_2(L^1)_2(\mu\text{-dppm})](ClO_4)_2$ illustrate a similar trend (Figure 10). A structureless band appears at λ_{max} = 640 nm for Pt_2, while a structured emission is observed at λ_{max} = 526 and 553 nm for Pd_2. The nature of the former is again ascribed to mixed d$\sigma^* \rightarrow \pi^*$/excimeric $\pi \rightarrow \pi^*$, while the excited state of the Pd_2 species is assigned as ^{3}IL accompanied by weak $\pi-\pi$ excimeric character.

Acknowledgment. We are grateful for financial support from The University of Hong Kong and the Research Grants Council of the Hong Kong SAR, China [HKU 7298/99P]. We thank Dr. V. M. Miskowski for helpful discussions.

Supporting Information Available: Listings of crystal data, atomic coordinates, calculated coordinates, anisotropic displacement parameters, and bond lengths and angles for **1d**(ClO_4), **1e**$(ClO_4)_2$·DMF, and **2e**$(ClO_4)_2$. This material is available free of charge via the Internet at http://pubs.acs.org.

IC991089G